Received 1 April 2022; accepted 9 May 2022. Date of publication 19 May 2022; date of current version 27 May 2022.
Digital Object Identifier 10.1109/OJAP.2022.3176399

Spatial Domain Indirect Holography for a Full Phaseless Approach to Biomedical Microwave Imaging

SANDRA COSTANZO [1,2,3,4] (Senior Member, IEEE), GIUSEPPE LOPEZ [1], AND GIUSEPPE DI MASSA [1] (Life Senior Member, IEEE)

[1] Department of Computer Engineering, Modeling, Electronics, and Systems Science (DIMES), University of Calabria, 87036 Rende, Italy
[2] National Research Council of Italy (CNR), Institute for Electromagnetic Sensing of the Environment (IREA), 80124 Naples, Italy
[3] Inter-University National Research Center on Interactions Between Electromagnetic Fields and Biosystems (ICEmB), 16145 Genoa, Italy
[4] Consorzio Nazionale Interuniversitario per le Telecomunicazioni, 43124 Parma, Italy

CORRESPONDING AUTHOR: S. COSTANZO (e-mail: costanzo@dimes.unical.it)

This work was supported in part by the European Social Fund (FSE) through the International Mobility Program of Ph.D. Students and Research Grants/Researchers of Type A—POR Calabria 2014–2020—Actions 10.5.6 and 10.5.12 and in part by the FESR-FSE 2014/2020, in the framework of NLHT (Nanoscience Laboratory for Human Technologies) Project.

ABSTRACT Microwave imaging approaches generally require the knowledge of the complex incident field distribution inside the imaging domain. This task can be accomplished by probing the observation domain, thus resulting in a time-consuming process, or assuming a numerical/simulated model. Alternatively, the incident field can be collected on the measurement domain, and the field distribution can be successfully retrieved on the whole imaging space. In this paper, a full phaseless, two-step strategy is described, where the phase of the incident field is retrieved by exploiting a spatial domain indirect holography technique, applied to the acquisition points only. The retrieved complex incident field can be so used for the reconstruction of the incident field inside the domain of interest. More specifically, a modal expansion technique and a source reconstruction method are adopted and compared to perform the above task. Once performing the characterization of the incident field distribution, the proposed strategy is included in the framework of a phaseless inverse scattering problem, where intensity-only data of the total field are involved. The effectiveness of the combined approach is demonstrated by considering an imaging scenario which involves a series of breast models as inhomogeneous targets.

INDEX TERMS Microwave imaging (MWI), incident field modeling, spatial domain holography, phase retrieval problem, phaseless microwave tomography.

I. INTRODUCTION

MICROWAVE imaging (MWI) techniques make use of electromagnetic inverse scattering solutions to reconstruct the features of a generic region of interest (ROI). Those different approaches include radar-based modalities, where only the target location can be determined, as well as qualitative and quantitative reconstructions – the former considering some restrictions on the physical properties of the object under test (OUT), e.g., limited size for the Born approximation, low-contrast compared to the background medium in the case of the Rytov approximation, or combination of both approaches, as recently provided in [1]. For what concerns the quantitative case, pertaining strategies aim at retrieve the dielectric profile of a certain object under test (OUT), limited within the imaging domain D. Generally speaking, the acquisition setup consists of a series of transmitters and receivers, located on a certain measurement domain S, where data are collected. Among the field captured in the presence of the target to be imaged, namely the total field, the (complex) distribution of the incident field, i.e., the field evaluated without the presence of the target, needs to be known. Apart from the knowledge of the incident field data on the domain S, the incident field distribution inside the domain D becomes crucial. On this context, the sampling of the whole domain D can be performed, resulting in a cumbersome measurement stage [2]. Therefore, rather than performing intensive measurements on the domain D, the incident field can be numerically modeled [3], [4], or, alternatively, it can be retrieved from measurements performed along S. Furthermore, phase measurements at microwave frequencies can suffer from poor accuracy, while phaseless near-field data result to be more robust with respect to probe positioning errors, in the case of a multi-view imaging system [5]. Performing a phase retrieval (PR) stage for the total field can be difficult to realize, when the measurement space data does not have enough cardinality to span the scattered field space. Furthermore, even if the inverse strategy, based on the prior estimation of the scattered field phase from amplitude-only data, allows a better control of the non-linearity [6], [7], an inverse single-step approach is preferred, since the errors in the phase computation of the total field could propagate to the second step, resulting in a non-linear amplification of such error. The authors believe that the PR stage, limited to the incident field modeling only, could not affect the overall reconstruction results, as compared to the case where the complex incident is supposed to be known.

According to the above statements, in this paper a full phaseless microwave imaging approach is described.

The proposed inverse scattering problem (ISP) involves two main steps:

1) the (complex) incident field distribution evaluation from amplitude-only data;
2) the effective inverse strategy, where the retrieved incident field data and the amplitude-only data of the total field are exploited.

Specifically, the paper mainly deals with the reconstruction method used for the incident field data evaluation, pertaining to the first step. The estimation of the incident field is based on a two-stage strategy, where, exploiting a spatial domain indirect holography technique (SDIHT), the incident field phase along the measurement points in S is retrieved first. Once the incident field is known in complex terms, two alternative approaches are investigated to retrieve the incident field distribution inside the imaging domain, namely the modal expansion (ME) technique and the source reconstruction method (SRM).

In the second step, the retrieved incident field is provided, together with amplitude-only data for the total field, and it is given as data input to a phaseless contrast source inversion method (P-CSI), validated for 2-D transverse magnetic (TM) scattering problems. The effectiveness of the full phaseless approach is investigated in the framework of an imaging scenario. Furthermore, an insight on the inherent phase retrieval capability of the method for the unused phase of the total field is described.

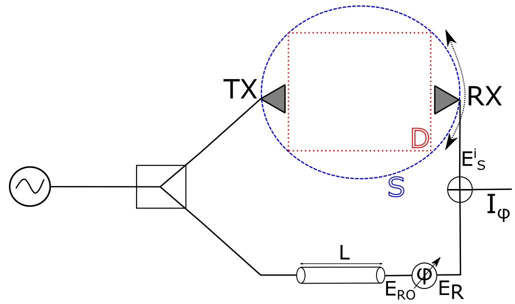

FIGURE 1. Spatial domain indirect holography technique (SDIHT) scheme, applied to a microwave imaging context, for the phase recovery of the incident field in the measurement domain.

II. METHODS AND PROCEDURES

A. SPATIAL DOMAIN INDIRECT HOLOGRAPHY TECHNIQUE (SDIHT) AS INCIDENT FIELD PHASE RETRIEVAL STRATEGY

As opposite to the standard direct holography, the indirect holographic approach assumes scalar near-field measurements; those intensity data are exploited to perform a phase retrieval step, thus recovering the complex near field distribution on the sampled points. Specifically, the SDIHT directly operates in the spatial domain, thus avoiding the spectral component analysis of the samples, as provided in [8]. Secondly, instead of performing measurements on two-planes, as conventionally done in other phase retrieval techniques [9]–[11] or alternatively by using two co-planar probes [12], the SDIHT approach performs a set of amplitude-only measurements for each probe location, by introducing a proper phase shift to the reference field data (Fig. 1). As opposed to the conventional holography pattern solution, which is derived starting from a scattered field sampling on the whole DOI, in this work the SDIHT is exploited as a phase retrieval method along the receiving points only.

As a matter of fact, the sampling in the SDIHT is limited to the acquisition curve S, where the transceivers are located. Then, for each transmitter location, the incident field values along the receiving points on S are retrieved, exploiting the SDIHT through amplitude-only measurements.

The use of this technique comes up to overcome a limitation of the imaging solution previously proposed by the authors, consisting of a phaseless inverse scheme based on the contrast source inversion method (P-CSI) [13], [14]. In the above method, the phaseless inverse scattering problem considers amplitude-only data for the total field, while assuming the knowledge of the incident field distribution in complex form, which is obtainable from measurements or numerical models. The latter assumptions are quite common in the microwave imaging context, where the incident field distribution is assumed as a system characterization, to be measured, or modeled, once and stored [15]–[17].

The use of the SDIHT, with a limited sample space, i.e., along the measurement curve S only, allows to realize a complete phaseless condition in the inverse scattering problem,

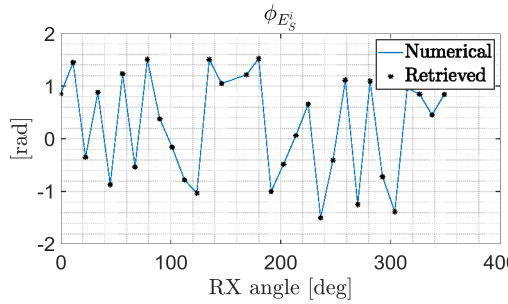

FIGURE 2. Spatial domain indirect holography technique (SDIHT) - retrieved phase vs. phase from the numerical model of the incident field, evaluated on the receivers' locations along the measurement curve S.

without performing a more dense near-field sampling of the incident field inside the DOI.

Accordingly, the estimation of the incident field within the imaging domain D is composed of two steps. Firstly, by applying the SDIHT, three squared amplitude measurements are performed, for three different phase values φ, imposed by the phase shifter along the feedback line (Fig. 1), for each transmitter-receiver couple. This measurement stage results in the following squared amplitude data:

$$I_\varphi = \left|E_S^i + E_R^\varphi\right|^2 = |E_S^i + E_{RO} \cdot e^{j\varphi}|^2 \text{ for } \varphi \in (-\pi/2, 0, \pi/2) \quad (1)$$

where E_{RO} is the reference signal, while E_S^i is the field coming from the receiving antenna. The squared amplitude signals I_φ are processed in order to retrieve the phase of the incident field, on a fixed receiver location, as detailed in [18]:

$$\tan^{-1}\left[\frac{(I_0 - I_{-\pi/2}) - (I_0 - I_{\pi/2})}{(I_0 - I_{-\pi/2}) + (I_0 - I_{\pi/2})}\right] = \phi_{E_S^i} - \phi_{E_{RO}} \quad (2)$$

where $\phi_{E_S^i}$ is the retrieved phase of the incident field, while $\phi_{E_{RO}}$ can be set by adjusting the cable length L. The measurements are performed for each transmitter and among the different receiver locations.

The SDIHT is tested by considering the incident field of a TMz line source, numerically represented in the form of a Hankel function of the second kind $-H_0^{(2)}$. The three squared amplitude signals are evaluated for each receiver position along S, while fixing the transmitter position (Fig. 1). The process is repeated for all the transmitter locations. The comparison between the phase of the numerical model and the retrieved phase values for a selected TX position, as a function of the RX angle, is shown in Fig. 2.

B. INCIDENT FIELD RECONSTRUCTION – MODAL EXPANSION (ME) TECHNIQUE

Once the complex incident field among S is retrieved, the incident field distribution within the imaging domain D needs to be found. The incident field distribution can be obtained by applying a modal expansion (ME) technique [19], [20]. For the case at hand, this task is accomplished by considering a polynomial expansion in terms of Hankel functions, namely:

$$E^i(r,\theta) = -\frac{j}{4}\sum_{n=-Nc}^{Nc} c_n H_n^{(2)}(k_b r)e^{jn\theta(r)} \quad (3)$$

where (r, θ) are the coordinates of the observation point with respect to the transmitter location, while k_b is the wavenumber in the background. The unknown c_n coefficients are preliminarily obtained by minimizing the squared distance between the field into Eq. (3) and the retrieved incident field along S. The truncation number N_c is properly chosen by following the specifics outlined in [19]. The least squares problem is solved through the use of the Singular Value Decomposition (SVD), applied to the following matrix form:

$$E_S^i = \mathbf{H}c \quad (4)$$

where $\mathbf{H}$ is the matrix including the Hankel functions. Once the expansion coefficients are known, the incident field in D -E_D^i- can be computed by using again Eq. (3), and considering the discretization grid nodes in D as observation points.

C. INCIDENT FIELD RECONSTRUCTION – SOURCE RECONSTRUCTION METHOD (SRM)

In alternative to the ME technique, once performing the SDIHT, a Source Reconstruction Method (SRM) can be exploited in order to obtain the incident field distribution in D, [21], [22]. Based on the equivalence principle, the SRM is an antenna diagnostics technique able to compute the current distributions, which are evaluated on a closed surface S' around the antenna under test (AUT), starting from a series of measurements performed on arbitrary point series. Once the equivalent currents are obtained, the radiated fields outside the equivalent current surface can be obtained by using a numerical forward solver. Generally speaking, for a fixed transmitting position, the electric field along the measurement curve S can be defined as:

$$E(\vec{r}) = E^{J_S}(\vec{r}) + E^{M_S}(\vec{r}) \quad (5)$$

where E^{J_S} is the field contribution due to the electric current density J_S, while E^{M_S} denotes the contribution coming from the magnetic current density M_S. In the case of TMz condition, the existence of the z-component of the electric current only - J_S^z - and the two orthogonal magnetic currents - M_S^x and M_S^y, allow us to express the corresponding contributions as [23], [24]:

$$E_z^{J_S^z}(\vec{r}) = -\frac{\omega\mu_0}{4}\int_{S'} J_S^z\left(\vec{r'}\right)H_0^{(2)}\left(k_b|\vec{r}-\vec{r'}|\right)dS' \quad (6)$$

$$E_z^{M_S^x}(\vec{r}) = -\frac{1}{4j}\int_{S'} M_S^x\left(\vec{r'}\right)k_b H_1^{(2)}\left(k_b|\vec{r}-\vec{r'}|\right)\frac{(y-y')}{|\vec{r}-\vec{r'}|}dS' \quad (7)$$

$$E_z^{M_S^y}(\vec{r}) = -\frac{1}{4j}\int_{S'} M_S^y\left(\vec{r'}\right)k_b H_1^{(2)}\left(k_b|\vec{r}-\vec{r'}|\right)\frac{(x-x')}{|\vec{r}-\vec{r'}|}dS' \quad (8)$$

TABLE 1. Incident field reconstruction – root mean square error (RMSE).

Reconstruction Method	RMSE	
	$\mathrm{Re}\{E_D^i\}$	$\mathrm{Im}\{E_D^i\}$
SDIHT + ME	0.0036	0.0028
SDIHT + SRM	0.0540	0.0461

Therefore, starting from the knowledge of the incident field in S, coming from the SDIHT stage, by combining the three contributions, the unknown equivalent currents can be found. This problem is solved by using a conjugate gradient least square method (CGLS) following the approach provided in [25]. Once the currents are known, the incident field distribution E_D^i inside the domain D can be computed according to the radiation operators in (6)-(8).

Before applying the ME or the SRM technique, the SDIHT data is corrupted with an additive noise, by using the following expression [26]:

$$E_S^{i_{noisy}} = E_S^i + \max\left(E_S^i\right)\frac{\eta}{\sqrt{2}}(\theta_1 + j\theta_2) \tag{9}$$

where θ_1,θ_2 are two real vectors, whose elements are random values uniformly distributed in the range $[-1, 1]$, while parameter η indicates the noise percentage. The reconstruction results coming from the ME and the SRM methods, with a 3% of noise, i.e., $\eta = 0.03$, are depicted in Fig. 3, and compared with the numerical model, for a certain transmitting location. The root mean square error (RMSE) is assumed as a quantitative metric for the reconstruction, whose results relative to the depicted case are listed in Table 1.

III. RESULTS

A. MWI RESULTS

Herein, the validity of the incident field reconstruction described in the previous section is analyzed within the regularized P-CSI iterative method for microwave tomography (MWT). The targets consist of a series of MRI-derived breast models [27], with different densities. For each model, a tumour inclusion has been added, as shown in the corresponding ground truth of Figs. 4(a)-7(a). The EM properties are imported according to the values obtained from the dielectric characterization of a set of realized mimicking-tissue phantoms for the involved tissues, as discussed in [28].

Each target is surrounded by 32 transceivers, displaced along the measurement domain S, with an operating frequency equal to 2 GHz, while immersed into a coupling medium with $\varepsilon_r = 18$ as relative permittivity, which is selected for the specific breast imaging case [29]. The incident field required by the inverse strategy is retrieved from one of the combined strategies presented in the previous sections. Specifically, since the SDIHT + ME and SDIHT + SRM exhibit similar performance in the incident field reconstruction for the case of a non-directive source,

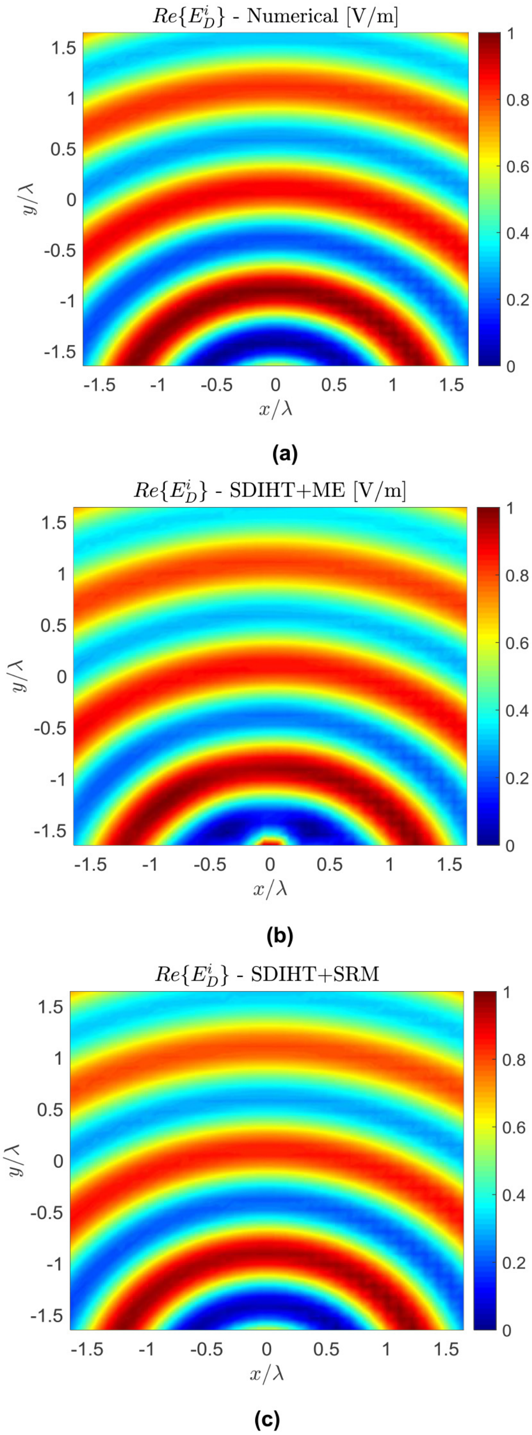

FIGURE 3. Example of incident field reconstruction - (a) numerical model, retrieved incident field in D in the case of (b) combined spatial domain indirect holography technique (SDIHT) and modal expansion (ME) and (c) SDIHT combined with the source reconstruction method (SRM). The normalized real part is shown.

the differences achieved in the imaging results by using the above two methods are not further investigated.

The synthetic total field data are numerically generated by using a forward solver based on the method of moments (MOM) [30], [31]. The phase of the total field

TABLE 2. Quantitative metrics for the different breast models.

Phantom ID	RMSE	ρ_{ε_r}
010204	8.77	0.897
012304	10.82	0.877
012204	8.14	0.904
071904	6.89	0.939

is neglected within the inverse strategy. Moreover, as highlighted by the authors in [32], [33], the cost function, which combines the contributions relative to the measured and the imaging domain, is defined in a compact form as [34]–[36]:

$$F\left(\chi^{(n)}\right) = \alpha_S \sum_{v=1}^{N_{TX}} \left|\left|r_{S,v}^{(n)}\right|\right|_S^2 + \alpha_D \sum_{v=1}^{N_{TX}} \left|\left|\rho_{D,v}^{(n)}\right|\right|_D^2 \quad (10)$$

where $r_{S,v}^{(n)}$ is the discrepancy in the S domain between the phaseless measured data and the correspondent scattering model, while $\rho_{D,v}^{(n)}$ includes the error affecting the scattering equation in the conventional complex form within D [35], whereas the terms α_{S-D} represent normalization factors.

Furthermore, a regularization layer is included, based on the total variation (TV) technique [37]. More specifically, the discrete version of the following operator is implemented in the contrast update stage [38]:

$$F_R(\chi) = \frac{1}{A} \int_D \frac{|\nabla \chi(r)|^2 + \delta^{(n)}}{\left|\nabla \chi^{(n)}(r)\right|^2 + \delta^{(n)}} dA \quad (11)$$

where A denotes the area of the imaging domain D, while $\delta^{(n)}$ is the steering parameter, responsible for the influence of the regularization as function of the number of iteration and set to $\delta^{(n)} = F(\chi^{(n)})/(\Delta x \Delta y)$, where $(\Delta x \Delta y)$ is the area of the single unit cell in the discretization grid. The iterative procedure is stopped if the maximum number of iterations is achieved or, alternatively, if the decrease in the cost function is less than 10^{-5} between two consecutive iterations.

The inversion strategy is tested for different inhomogeneity levels of the breast targets. The corresponding reconstructed real permittivity profiles are shown in Figs. 4(b)-7(b).

The quantitative aspects of the permittivity versus the ground truth data are evaluated with a series of standard error criterion. For the case at hand, the RMSE for the relative permittivity is evaluated with reference to the considered targets [39].

As a second metric, the cross-correlation coefficient ρ_{ε_r} is used to qualitatively estimate the similarity between the actual and the reconstruction quantities. In the case of the dielectric contrast, this can be defined as:

$$\rho_{\varepsilon_r} = \frac{\varepsilon_{r_{true}} \cdot \varepsilon_{r_{est}}}{\left|\varepsilon_{r_{true}}\right| \cdot \left|\varepsilon_{r_{est}}\right|} \quad (12)$$

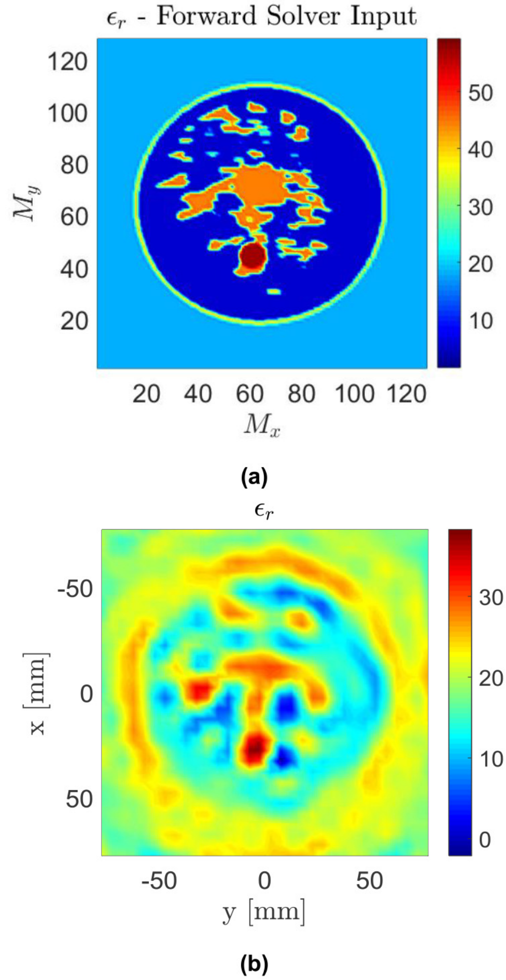

FIGURE 4. Phantom ID: 010204 – Ground truth (a) and reconstructed real permittivity (b).

The two above-mentioned metrics, evaluated for the different reconstructed targets, are summarized in Table 2. The values of the metrics shows that the P-CSI, with the inclusion of the incident field strategy from phaseless data, provides good cross-correlation results, with a reduced accuracy in terms of RMSE. At this stage, the method is able to identify the abrupt permittivity variations, i.e., localizing the region with a high contrast, while the reconstruction is less quantitatively accurate in the case of low-contrast portions, such as the malignant-modeled region within the fibroglandular tissue. This limitations comes from the nature of the CSI itself, while the SDIHT-based reconstruction methods for the incident field does not impact on the quantitative reconstruction capabilities of the method.

B. A SIDE NOTE ON THE PHASE RETRIEVAL CAPABILITY OF THE P-CSI METHOD

Apart from the analysis of the electromagnetic properties reconstruction, the authors want to highlight an additive peculiarity of the phaseless reconstruction method. Let us consider the contribution of the cost function used in the

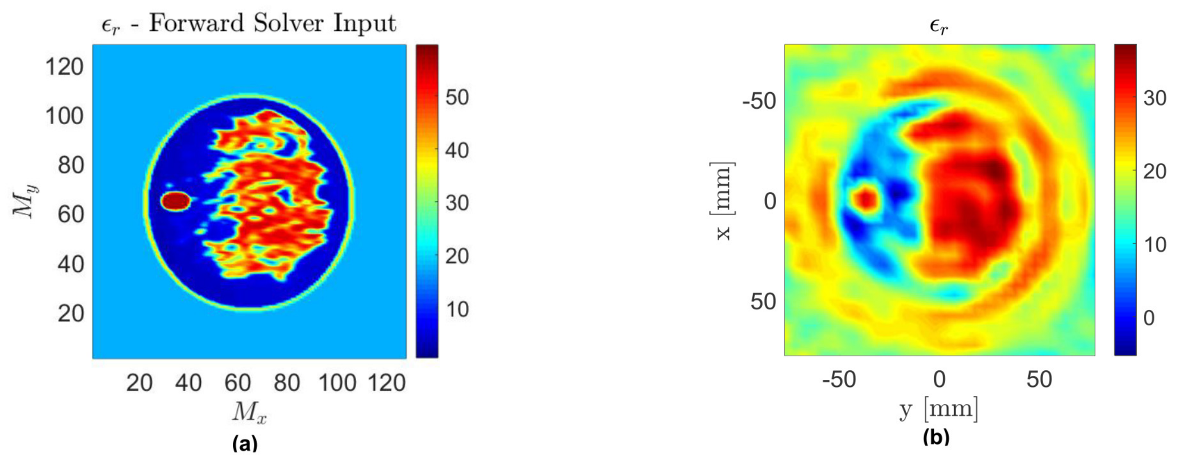

FIGURE 5. Phantom ID: 012304 – Ground truth (a) and reconstructed real permittivity (b).

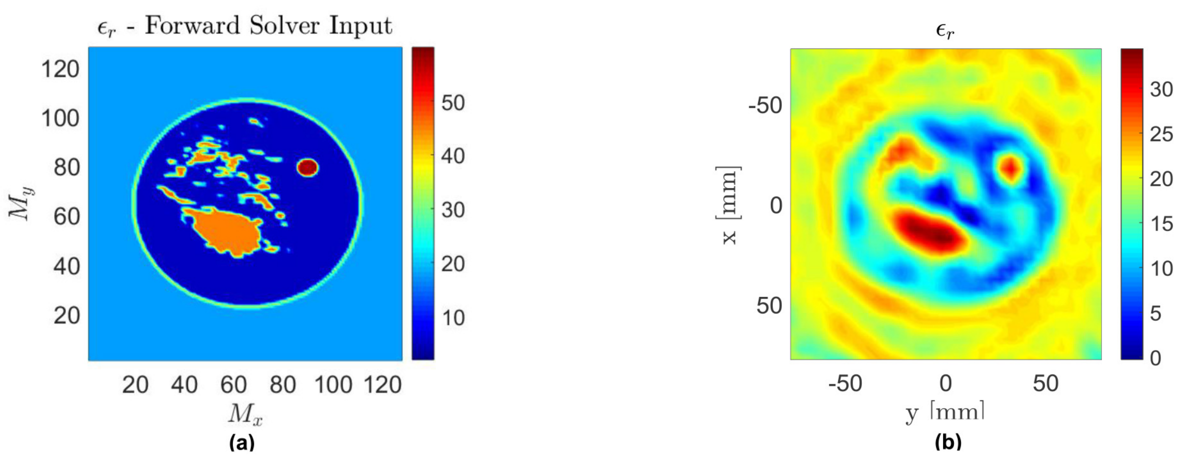

FIGURE 6. Phantom ID: 012204 – Ground truth (a) and reconstructed real permittivity (b).

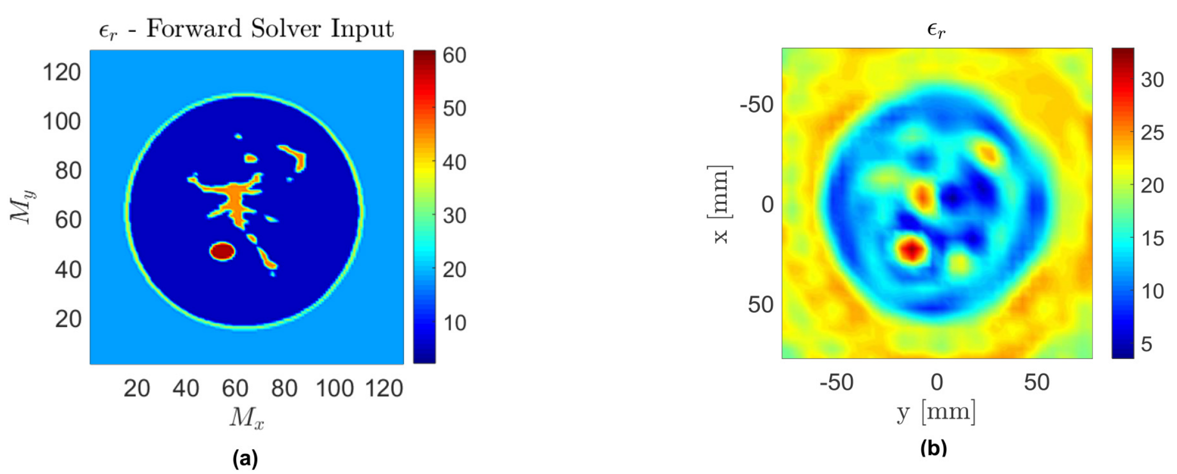

FIGURE 7. Phantom ID: 071904 – Ground truth (a) and reconstructed real permittivity (b).

iterative scheme, and relative to the phaseless data samples only, namely:

$$F_S(\omega_v^{(n)}) = \alpha_S \sum_{v=1}^{N_{TX}} \left|\left| r_{S,v}^{(n)} \right|\right|_S^2 \tag{13}$$

The term $r_{S,v}^{(n)}$ into Eq. (13) gives the residual, defined as:

$$r_{S,v}^{(n)} = \left|E_{S,v}^{tot}\right|^2 - \left|E_{S,v}^{tot-model}\right|^2 \tag{14}$$

It indicates the discrepancy between the measured intensity of the total field $|E_{S,v}^{tot}|$, and the corresponding value, obtained from the reconstruction model, $|E_{S,v}^{tot-model}|$.

For the latter, according to the scattering problem, we have:

$$E_{S,v}^{tot-model} = E_{S,v}^{inc} + G_S \omega_v \tag{15}$$

where ω_v is the contrast source obtained at the end of the iteration, while the parameter v denotes the vth transmitter location along the acquisition curve, and G_S is the Green's operator involving the measurement points on S.

The gradient relative to the cost function into Eq. (13), used in the conjugate gradient scheme for the contrast source (CS) update and calculated through the Fréchet derivative, at the nth iteration, results to be:

$$g_{S,v}^{(n)} = G_S^* \left[2E^{tot-model(n-1)} r_{S,v}^{n-1} \right] \tag{16}$$

where [*] denotes the adjoint operator. Eq. (16) clearly shows that the approximation of the total field coming from the model is included within the residual error calculation. The discrepancy between the retrieved total field at the end of the iteration process, and the total field coming from the forward solver – for which the phase content has been neglected in the inversion strategy - is shown in Fig. 8. This is relative to the last analyzed breast case, for all the TX-RX pairs, in terms of both amplitude and phase. Similar results can be obtained for the remaining test-cases. Consequently, if the convergence is achieved, also the total field, in its complex form, is implicitly retrieved within the CS update stage. Therefore, the lack of the measured phase information of the total field, due to the phaseless approach, results to be compensated within the iterative update procedure of the contrast source, by exploiting the modeled (and not measured) total field in its complex form, namely $E^{tot-model}$.

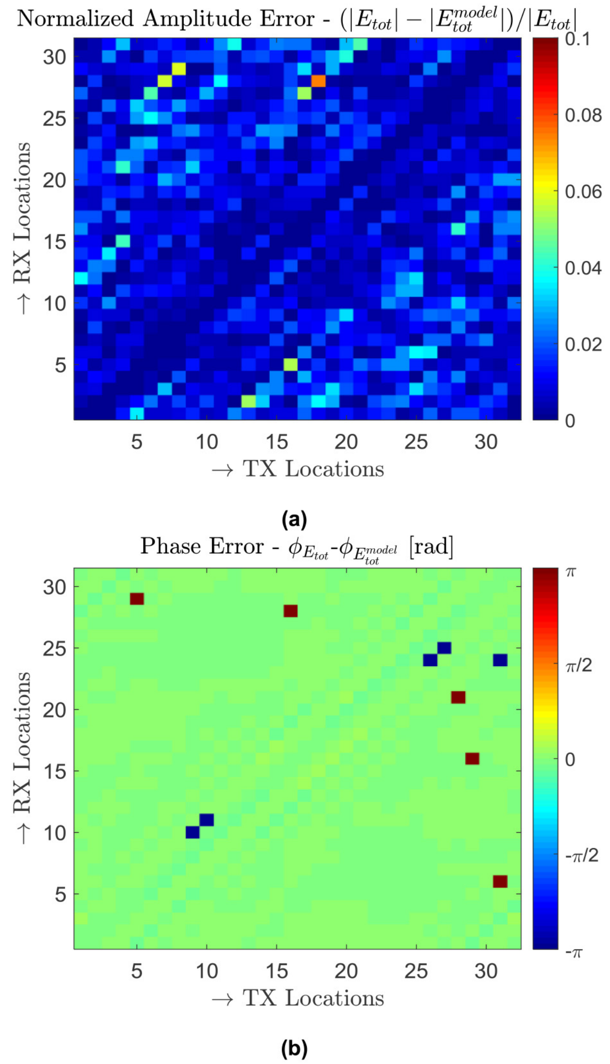

FIGURE 8. **Reconstruction Errors for the total field at the end of the iterations – Normalized Amplitude Error (a) and Phase Error (b).**

IV. CONCLUSION

In this contribution, a spatial domain phase retrieval technique has been exploited for microwave imaging purposes. Originally proposed for holography applications, the above technique has been used to retrieve the phase of the incident field, starting from intensity-only data, which are evaluated along the measurement domain. Once the incident field is retrieved in its complex form, a modal expansion technique or, alternatively, a source reconstruction method, has been used to reconstruct the complex incident field in the imaging domain. The retrieved incident field quantities are then included within a phaseless inverse scattering method, in which a phaseless acquisition of the total field is adopted to recover the electromagnetic properties of the target under test. Consequently, the combined approach suggests the potential usage of amplitude-only data for imaging applications. As future investigations, the extension of the proposed method to realistic 3D breast imaging will be considered. Furthermore, even if actually applied to simple TMz line sources, the extension of the outlined approach will be considered in the case of incident field reconstruction for realistic antennas with specific shape and near-field distribution.

REFERENCES

[1] D. Tajik, R. Kazemivala, and N. K. Nikolova, "Real-time imaging with simultaneous use of born and Rytov approximations in quantitative microwave holography," *IEEE Trans. Microw. Theory Techn.*, vol. 70, no. 3, pp. 1896–1909, Mar. 2022, doi: 10.1109/TMTT.2021.3131227.

[2] T. Henriksson, N. Joachimowicz, C. Conessa, and J.-C. Bolomey, "Quantitative microwave imaging for breast cancer detection using a planar 2.45 GHz system," *IEEE Trans. Instrum. Meas.*, vol. 59, no. 10, pp. 2691–2699, Oct. 2010, doi: 10.1109/TIM.2010.2045540.

[3] L. Crocco, M. D'Urso, and T. Isernia, "Inverse scattering from phaseless measurements of the total field on a closed curve," *J. Opt. Soc. Amer. A*, vol. 21, no. 4, pp. 622–631, Apr. 2004, doi: 10.1364/JOSAA.21.000622.

[4] G. Franceschini, M. Donelli, R. Azaro, and A. Massa, "Inversion of phaseless total field data using a two-step strategy based on the iterative multiscaling approach," *IEEE Trans. Geosci. Remote Sens.*, vol. 44, no. 12, pp. 3527–3539, Dec. 2006, doi: 10.1109/TGRS.2006.881753.

[5] S. F. Razavi and Y. Rahmat-Samii, "Resilience to probe-positioning errors in planar phaseless near-field measurements," *IEEE Trans. Antennas Propag.*, vol. 58, no. 8, pp. 2632–2640, Aug. 2010, doi: 10.1109/TAP.2010.2050421.

[6] L. Crocco, M. D'Urso, and T. Isernia, "Faithful non-linear imaging from only-amplitude measurements of incident and total fields," *Opt. Exp.*, vol. 15, no. 7, pp. 3804–3815, Apr. 2007, doi: 10.1364/OE.15.003804.

[7] M. D'Urso, K. Belkebir, L. Crocco, T. Isernia, and A. Litman, "Phaseless imaging with experimental data: Facts and challenges," *J. Opt. Soc. Amer. A*, vol. 25, no. 1, pp. 271–281, Jan. 2008, doi: 10.1364/JOSAA.25.000271.

[8] S. Costanzo and G. Di Massa, "Microwave imaging with spatial-domain indirect holography," in *Proc. 19th Int. Conf. Electromagn. Adv. Appl. (ICEAA)*, Oct. 2017, pp. 1412–1414, doi: 10.1109/ICEAA.2017.8065543.

[9] T. Brown, I. Jeffrey, and P. Mojabi, "Multiplicatively regularized source reconstruction method for phaseless planar near-field antenna measurements," *IEEE Trans. Antennas Propag.*, vol. 65, no. 4, pp. 2020–2031, Apr. 2017, doi: 10.1109/TAP.2017.2670518.

[10] A. P. Anderson and S. Sali, "New possibilities for phaseless microwave diagnostics. Part1: Error reduction techniques," *IEE Proc. H, Microw. Opt. Antennas*, vol. 132, no. 5, pp. 291–298, 1985, doi: 10.1049/IP-H-2.1985.0053.

[11] T. Isernia, G. Leone, and R. Pierri, "Radiation pattern evaluation from near-field intensities on planes," *IEEE Trans. Antennas Propag.*, vol. 44, no. 5, pp. 701–710, May 1996, doi: 10.1109/8.496257.

[12] S. Costanzo and G. Di Massa, "An integrated probe for phaseless near-field measurements," *Measurement*, vol. 31, no. 2, pp. 123–129, Mar. 2002, doi: 10.1016/S0263-2241(01)00036-7.

[13] S. Costanzo and G. Lopez, "Low-complexity amplitude-only breast imaging technique," in *Proc. 15th Eur. Conf. Antennas Propag. (EuCAP)*, Mar. 2021, pp. 1–5, doi: 10.23919/EuCAP51087.2021.9411423.

[14] S. Costanzo and G. Lopez, "Phaseless approach to microwave biomedical imaging: System requirements towards clinical applications," in *Proc. 14th Eur. Conf. Antennas Propag. (EuCAP)*, Mar. 2020, pp. 1–4, doi: 10.23919/EuCAP48036.2020.9136069.

[15] O. M. Bucci, L. Crocco, M. D'Urso, and T. Isernia, "Inverse scattering from phaseless measurements of the total field on open lines," *J. Opt. Soc. Amer. A, Opt. Image Sci. Vis.*, vol. 23, no. 10, pp. 2566–2577, Oct. 2006.

[16] C. Narendra and P. Mojabi, "Phaseless Gauss–Newton inversion for microwave imaging," *IEEE Trans. Antennas Propag.*, vol. 69, no. 1, pp. 443–456, Jan. 2021, doi: 10.1109/TAP.2020.3026427.

[17] C. Estatico, A. Fedeli, M. Pastorino, A. Randazzo, and E. Tavanti, "A phaseless microwave imaging approach based on a Lebesgue-space inversion algorithm," *IEEE Trans. Antennas Propag.*, vol. 68, no. 12, pp. 8091–8103, Dec. 2020, doi: 10.1109/TAP.2020.2999789.

[18] S. Costanzo and G. Di Massa, "Spatial domain indirect holographic technique for antenna near-field phaseless measurements," *Radio Sci.*, vol. 52, no. 4, pp. 432–438, Apr. 2017, doi: 10.1002/2016RS006154.

[19] T. Tsuburaya, Z. Meng, and T. Takenaka, "Inverse scattering analysis from measurement data of total electric and magnetic fields by means of cylindrical-wave expansion," *Electronics*, vol. 8, no. 4, p. 417, Apr. 2019, doi: 10.3390/electronics8040417.

[20] D. Colton and R. Kress, *Inverse Acoustic and Electromagnetic Scattering Theory*, vol. 93. Berlin, Germany: Springer, 1998, doi: 10.1007/978-3-662-03537-5.

[21] T. K. Sarkar, M. Salazar-Palma, M. D. Zhu, and H. Chen, "The source reconstruction method," in *Modern Characterization of Electromagnetic Systems and its Associated Metrology*. Hoboken, NJ, USA: IEEE, 2021, pp. 235–317, doi: 10.1002/9781119076230.ch5.

[22] Y. Alvarez, F. Las-Heras, and M. R. Pino, "Reconstruction of equivalent currents distribution over arbitrary three-dimensional surfaces based on integral equation algorithms," *IEEE Trans. Antennas Propag.*, vol. 55, no. 12, pp. 3460–3468, Dec. 2007, doi: 10.1109/TAP.2007.910316.

[23] C. Narendra, I. Jeffrey, and P. Mojabi, "Using the source reconstruction method to model incident fields in microwave tomography," *IEEE Antennas Wireless Propag. Lett.*, vol. 16, pp. 46–49, 2017, doi: 10.1109/LAWP.2016.2554059.

[24] Y. A. Lopéz, F. L.-H. Andrés, M. R. Pino, and T. K. Sarkar, "An improved super-resolution source reconstruction method," *IEEE Trans. Instrum. Meas.*, vol. 58, no. 11, pp. 3855–3866, Nov. 2009, doi: 10.1109/TIM.2009.2020847.

[25] P. C. Hansen, "REGULARIZATION TOOLS: A MATLAB package for analysis and solution of discrete ill-posed problems," *Numer. Algorithms*, vol. 6, no. 1, pp. 1–35, Mar. 1994, doi: 10.1007/BF02149761.

[26] A. Abubakar, P. M. Van den Berg, and S. Y. Semenov, "A robust iterative method for born inversion," *IEEE Trans. Geosci. Remote Sens.*, vol. 42, no. 2, pp. 342–354, Feb. 2004, doi: 10.1109/TGRS.2003.821062.

[27] M. J. Burfeindt *et al.*, "MRI-derived 3-D-printed breast phantom for microwave breast imaging validation," *IEEE Antennas Wireless Propag. Lett.*, vol. 11, pp. 1610–1613, 2012, doi: 10.1109/LAWP.2012.2236293.

[28] S. Costanzo and G. Lopez, "Dielectric characterization of breast phantoms for phaseless microwave imaging focused on tumor identification," in *Trends and Applications in Information Systems and Technologies* (Advances in Intelligent Systems and Computing, 1368). Cham, Switzerland: Springer, 2021, pp. 248–254, doi: 10.1007/978-3-030-72654-6_24.

[29] P. M. Meaney, C. J. Fox, S. D. Geimer, and K. D. Paulsen, "Electrical characterization of glycerin: Water mixtures: Implications for use as a coupling medium in microwave tomography," *IEEE Trans. Microw. Theory Techn.*, vol. 65, no. 5, pp. 1471–1478, May 2017, doi: 10.1109/TMTT.2016.2638423.

[30] Y. Qin, T. Rodet, M. Lambert, and D. Lesselier, "Microwave breast imaging with prior ultrasound information," *IEEE Open J. Antennas Propag.*, vol. 1, pp. 472–482, 2020, doi: 10.1109/ojap.2020.3019953.

[31] Z. Wei and X. Chen, "Deep-learning schemes for full-wave nonlinear inverse scattering problems," *IEEE Trans. Geosci. Remote Sens.*, vol. 57, no. 4, pp. 1849–1860, Apr. 2019, doi: 10.1109/TGRS.2018.2869221.

[32] S. Costanzo and G. Lopez, "Phaseless microwave tomography assessment for breast imaging: Preliminary results," *Int. J. Antennas Propag.*, vol. 2020, Feb. 2020, Art. no. 5780243, doi: 10.1155/2020/5780243.

[33] S. Costanzo and G. Lopez, "Phaseless single-step microwave imaging technique for biomedical applications," *Radioengineering*, vol. 28, no. 3, pp. 512–516, 2019, doi: 10.13164/re.2019.0512.

[34] L. Li, H. Zheng, and F. Li, "Two-dimensional contrast source inversion method with phaseless data: TM case," *IEEE Trans. Geosci. Remote Sens.*, vol. 47, no. 6, pp. 1719–1736, Jun. 2009, doi: 10.1109/TGRS.2008.2006360.

[35] P. M. van den Berg, *Forward and Inverse Scattering Algorithms Based on Contrast Source Integral Equations*. Hoboken, NJ, USA: Wiley, 2021, doi: 10.1002/9781119741602.

[36] A. Arduino, O. Bottauscio, M. Chiampi, and L. Zilberti, "Magnetic resonance-based imaging of human electric properties with phaseless contrast source inversion," *Inverse Problems*, vol. 34, no. 8, Aug. 2018, Art. no. 84002, doi: 10.1088/1361-6420/aac536.

[37] A. Abubakar, P. M. Van Den Berg, and T. M. Habashy, "Application of the multiplicative regularized contrast source inversion method on TM- and TE-polarized experimental Fresnel data," *Inverse Problems*, vol. 21, no. 6, p. S5, Dec. 2005, doi: 10.1088/0266-5611/21/6/S02.

[38] P. M. van den Berg, *Forward and Inverse Scattering Algorithms Based on Contrast Source Integral Equations*. Hoboken, NJ, USA: Wiley, 2021, doi: 10.1002/9781119741602.

[39] F. Gao, B. D. Van Veen, and S. C. Hagness, "Sensitivity of the distorted born iterative method to the initial guess in microwave breast imaging," *IEEE Trans. Antennas Propag.*, vol. 63, no. 8, pp. 3540–3547, Aug. 2015, doi: 10.1109/TAP.2015.2436406.

SANDRA COSTANZO (Senior Member, IEEE) received the Laurea Degree (*summa cum laude*) in computer engineering from the Università della Calabria, Italy, in 1996, and the Ph.D. degree in electronic engineering from the Università Mediterranea di Reggio Calabria, Italy, in 2000. In 2017, she awarded the Italian National Scientific Qualification for the Full Professor position. Since 2019, she has been Associate with IREA-CNR, Naples. She is currently an Associate Professor with the Università della Calabria, where she is the Coordinator of Master's Degree of Telecommunication Engineering and the Rector's Delegate for Security, Protection and Control of Electromagnetic Fields. She teaches courses on electromagnetic waves propagation, antennas, remote sensing, radar, sensors, and electromagnetic diagnostics. She has authored or coauthored over 200 contributions in international journals, books, and conferences. Her research interests are focused on near-field/far-field techniques, antenna measurement techniques, antenna analysis and synthesis, numerical methods in electromagnetics, millimeter wave antennas, reflectarrays, synthesis methods for microwave structures, electromagnetic characterization of materials, biomedical applications, and radar technologies. She received the Telecom Prize for the Best Laurea Thesis in 1996 and the Best Academia and Research Application in Aerospace and Defense 2013 Award for the application Software Defined Radar using the NI USRP 2920 platform. She is an Associate Editor of IEEE ACCESS, IEEE JOURNAL OF ELECTROMAGNETICS, RF AND MICROWAVES IN MEDICINE AND BIOLOGY, and Electronics (section "Microwave and Wireless Communications") and a Editorial Board Member of *Radioengineering* and *International Journal of RF and Microwave Computer-Aided Engineering*. She is an Editor of the books *Microwave Materials Characterization* (INTECH) in 2012 and *Wave Propagation Concepts for Near-Future Telecommunication Systems* (INTECH) in 2017. She was a Lead Editor of Special Issues titled: Reflectarray Antennas: Analysis and Synthesis Techniques in 2012, Advances in Radar Technologies in 2013, Compressed Sensing: Applications in Radar and Communications in 2016, Bioengineering Applications of Electromagnetic Wave Propagation in 2019, and "Microwave Sensors for Biomedical Applications" in 2020. She is a member of the IEEE MTT-28 Biological Effects and Medical Applications Committee, IEEE South Italy Geoscience and Remote Sensing Chapter, Consorzio Nazionale Interuniversitario per le Telecomunicazioni, Società Italiana di Elettromagnetismo, and Centro Interuniversitario sulle Interazioni fra Campi Elettromagnetici e Biosistemi (ICEMB) and a Board Member of the IEEE AP/ED/MTT North Italy Chapter.

GIUSEPPE LOPEZ received the bachelor's degree (*summa cum laude*) in electronic engineering and the master's degree (*summa cum laude*) in telecommunications engineering from the University of Calabria, Italy, in 2016 and 2019, respectively, where he is currently pursuing the Ph.D. degree in information and communication technologies. His research activity is mainly focused on radar technologies, antenna design, microwave imaging techniques, computational electromagnetics, electromagnetic inverse scattering, and dielectric material characterization.

GIUSEPPE DI MASSA (Life Senior Member, IEEE) was born in Barano d'Ischia, Naples, Italy, in 1948. He received the Laurea degree in electronic engineering from the Università di Napoli Federico II, Naples, in 1973, where he was a Professor of Antennas from 1978 to 1979. In 1980, he joined the Università della Calabria, Italy, as a Professor of Electromagnetic Waves. Since 1985, he has been an Associate Professor and has been a Full Professor since 1994 with the Università della Calabria, where he teaches antennas and electromagnetic fields. From 1985 to 1986, he was a Scientific Associate with CERN, Geneva. In 1988, he was a Visiting Professor with the Brookhaven National Laboratory, Long Island, NY, USA. From 1997 to 2002, he was the Dean of the Department of Elettronica, Informatica and Sistemistica and the President of Programming Committee with the Università della Calabria. From 2000 to 2017, he was the Chairman of the Telecommunication Engineering Program with the Università della Calabria. He has authored/coauthored over 350 scientific articles, mainly on international scientific journals or proceedings of international conferences. He is the Principal Investigator or a Coordinator of many research programs, granted by national and international research organizations, as well as by leading national companies. He was the Italian Delegate in the European COST 284 Innovative Antennas for Emerging Terrestrial and Space-Based Applications, from 2002 to 2006 and from 2007 to 2011, in the COST Action IC0603: Antenna Systems and Sensors for Information Society Technologies. From 2003 to 2007, he participated in the Network of Excellence Antenna Center of Excellence, where he was the part of the Governing Board and the Leader of Work Group WP 1.2-1: Antenna Measurement Services. From 2011 to 2014, he was the Italian Delegate in the Management Committee of the COST Action IC1102, Versatile Integrated, and Signal-Aware Technologies for Antennas. Since 2019, he has been a Emeritus Professor with Università della Calabria. His main research interests include applied computational electromagnetics, microstrip antennas, microwave integrated circuits, reflectarrays, Gaussian beam solutions, millimeter wave antennas, near-field measurements, electromagnetic characterization of materials, and innovative radar antennas and technologies.